CANCER COMMUNICATIONS
Open Access

ORIGINAL ARTICLE

miR-495 and miR-5688 are down-regulated in non-small cell lung cancer under hypoxia to maintain interleukin-11 expression

Meng Zhao[1],[*] | Jiao Chang[1],[*] | Ran Liu[2] | Yahui Liu[1] | Jin Qi[3] |
Yanhui Wang[1] | Xinwei Zhang[1] | Lu Qiao[1] | Yu Jin[1] | Haohua An[1] | Li Ren [1] (ORCID)

[1] Department of Clinical Laboratory, Tianjin Medical University Cancer Institute and Hospital, National Clinical Research Center for Cancer, Key Laboratory of Cancer Prevention and Therapy, Tianjin's Clinical Research Center for Cancer, National Human Genetic Resources Sharing Service Platform, Tianjin 300060, P. R. China

[2] Department of Immunology, Tianjin Key Laboratory of Cellular and Molecular Immunology, Key Laboratory of Educational Ministry of China, School of Basic Medical Sciences, Tianjin Medical University, Tianjin 300070, P. R. China

[3] Department of Radiology, Tianjin Medical University Cancer Institute and Hospital, National Clinical Research Center for Cancer, Key Laboratory of Cancer Prevention and Therapy, Tianjin's Clinical Research Center for Cancer, National Human Genetic Resources Sharing Service Platform, Tianjin 300060, P. R. China

Correspondence
Li Ren, Tianjin Medical University Cancer Institute and Hospital, Huanhuxi Road, Tiyuanbei, Hexi District, Tianjin 300060, P. R. China.
Email: lirentmu@163.com

*These authors contributed equally to this work

Funding information
National Natural Science Foundation of China, Grant/Award Number: 81602026; Natural Science Foundation of Tianjin, Grant/Award Numbers: 18JCQNJC81600, 18JCZDJC32600

Abstract

Background: Hypoxia is a hallmark of cancer and is associated with poor prognosis. However, the molecular mechanism by which hypoxia promotes tumor progression remains unclear. MicroRNAs dysregulation has been shown to play a critical role in the tumor and tumor microenvironment. Here, we investigated the roles of miR-495 and miR-5688 in human non-small cell lung cancer (NSCLC) and their underlying mechanism.

Methods: The expression levels of miR-495 and miR-5688 in human NSCLC tissue specimens were measured by quantitative real-time polymerase chain reaction (qRT-PCR). Deferoxamine (DFO) was used to determine whether the regulation of miR-495 and miR-5688 under hypoxia was dependent on hypoxia-inducible factor 1-alpha (HIF-1α). Furthermore, the functions of miR-495 and miR-5688 in tumor progression were evaluated using colony formation, 3-(4,5-dimethylthiazol-2-yl)-5-(3-carboxymethoxyphenyl)-2-(4-sulfophenyl)-2H-tetrazolium (MTS), wound healing, transwell assays, and xenograft model. Two algorithms, PicTAR and Targetscan, were used to predict the target gene of these two miRNAs, and dual-luciferase reporter assay was conducted to confirm the target. The unpaired two-tailed t test, Pearson correlation analysis, and Fisher's exact probability test were performed for statistical analyses.

Results: Two miRNAs, miR-495 and miR-5688, were found to participate in NSCLC progression under hypoxia. They were down-regulated in NSCLC tissues compared with normal tissues. We determined that hypoxia led to the

down-regulation of miR-495 and miR-5688 in NSCLC cells, which was independent of HIF-1α and cellular metabolic energy. In addition, miR-495 and miR-5688 suppressed cell proliferation, migration, and invasion *in vitro*. The NSCLC xenograft model showed that miR-495 and miR-5688 inhibited tumor formation *in vivo*. Interestingly, we found that miR-495 and miR-5688 had the same target, interleukin-11 (IL-11). Recombinant human IL-11 counteracted the effects of miR-495 and miR-5688 on NSCLC cells, suggesting that miR-495 and miR-5688 executed their tumor suppressive role by repressing IL-11 expression.

Conclusion: We found that hypoxia down-regulated the expression levels of miR-495 and miR-5688 in NSCLC to enhance IL-11 expression and tumor progression, indicating that the miR-495/miR-5688/IL-11 axis may serve as a therapeutic target and potential biomarker for NSCLC.

1 | BACKGROUND

The tumor microenvironment refers to the surrounding microenvironment in which tumor cells are present, consisting of stromal cells, extracellular matrix, and signaling molecules that communicate with cancer cells [1]. The tumor microenvironment dictates the fate of tumor cells and plays a critical role in the subsequent development of malignancies [2]. Tumor growth and metastasis are highly dependent on interactions between the tumor and the associated microenvironment [3]. Hypoxia is a common phenomenon occurring in the majority of tumors and has been demonstrated to play an important role in tumor progression [4]. Decreased oxygen tension in tissues below physiological requirements induces hypoxic adaptive responses, which are regulated by a variety of transcription factors and signaling proteins [5]. The hypoxia-inducible factor (HIF) is the "master" regulator of these responses [6]. In addition, hypoxia induces strong changes in cell metabolism, gene expression, function, and so on. Therefore, understanding the mechanism by which hypoxia promotes tumor progression may help to develop treatment strategies for tumors at specific stages of development.

Lung cancer is a common malignant tumor in the world, with the highest incidence in men and the second highest incidence in women [7]. Non-small cell lung cancer (NSCLC) accounts for approximately 80% of all lung cancers and is classified as squamous cell carcinoma, adenocarcinoma, and large cell carcinoma [8]. Most of the patients are diagnosed at an advanced stage, and the 5-year survival rate is low (approximately 17.4%) [9]. The main treatments for NSCLC are surgery, radiotherapy, and chemotherapy, but the efficacy is limited for advanced stages [10]. In addition, the molecular mechanisms underlying NSCLC development have yet to be fully elucidated [11]. The exploration of molecular mechanism may help develop targeted therapy, a new treatment option for advanced NSCLC, which can not only improve treatment efficacy but also reduce some adverse effects [12]. Therefore, the molecular mechanisms of NSCLC initiation and progression should be further investigated to establish novel prognostic biomarkers and therapeutic methods for patients with this disease.

MicroRNAs (miRNAs) are a class of non-coding RNAs, approximately 22 nucleotides in length, that regulate gene expression by incomplete complementarity with the 3′-untranslated region (3′-UTR) of the target gene mRNA and therefore stimulate mRNA degradation or translational inhibition [13]. miRNA dysregulation has been demonstrated to be involved in various cellular biological processes, including cell proliferation, cell cycle, apoptosis, angiogenesis, invasion, migration, epithelial-to-mesenchymal transition, and metastasis [14]. Many studies have shown that miRNAs can play a role as promoters or inhibitors in the occurrence and development of tumors [15]. miR-495 is abnormally expressed in multiple types of human cancers. For example, it is up-regulated in bladder cancer [16] and down-regulated in gastric cancer [3], lung cancer [11], hepatocellular carcinoma [17], and breast cancer [18]. Although miR-495 was reported to be down-regulated in NSCLC, the expression level and roles of miR-5688, which is located in the same cluster as miR-495, have yet to be completely elucidated in NSCLC.

Interleukin-11 (IL-11) is a cytokine in the chemokine family that plays an important role in transmitting

information, activating and regulating immune cells, and mediating the differentiation of T/B cells and inflammatory response [19]. Previous studies have shown that IL-11 was abnormally expressed in many solid tumors and was related to the tumor microenvironment [20]. Furthermore, our previous research findings showed that IL-11 functioned as a prominent pro-tumorigenic cytokine in NSCLC by activating the signal transducer and activator of transcription 3 (STAT3) and AKT pathways [21]. Therefore, inhibiting IL-11 signaling might be a promising therapeutic strategy for the treatment of NSCLC. However, IL-11 inhibitors involved in NSCLC have been poorly defined.

In this study, we aimed to explore the molecular mechanism of NSCLC and identify potential therapeutic and diagnostic targets for it. Therefore, we detected the expression of miR-495 and miR-5688 in NSCLC and explored their functions and specific mechanisms.

2 | MATERIALS AND METHODS

2.1 | Cell culture and reagents

The human non-small cell lung adenocarcinoma cell lines A549 and H1299 were obtained from the American Type Culture Collection. The A549 cell line was established through explant culture of lung carcinomatous tissue, which could synthesize lecithin with a high percentage of disaturated fatty acids using the cytidine diphosphocholine pathway. The H1299 cell line was established from a lymph node metastasis of the lung from a patient who had received prior radiotherapy, which have a homozygous partial deletion of the p53 protein, and lack expression of p53 protein. A549 and H1299 cells were cultured in RPMI-1640 (Gibco, Rockville, MD, USA) supplemented with 10% fetal bovine serum (FBS, Gibco) and maintained at 37°C in a humidified atmosphere with 5% CO_2. Hypoxic cell culture (0.5% O_2) was achieved by putting cells in a hypoxia incubator filled with a mix of 0.5% O_2, 5% CO_2, and 94.5% N_2. The protein expression of HIF-1α under hypoxia was detected to prove the success of hypoxia. In addition, the mRNA expression levels of miR-495, miR-5688, and IL-11 and the secreted protein level of IL-11 under hypoxia were examined. Deficiencies of glucose and glutamine were achieved by culturing the cells with glucose-free medium (Gibco) and glutamine-free medium (Sigma-Aldrich, St. Louis, MO, USA).

A549 and H1299 cells were treated with deferoxamine (DFO; Sigma-Aldrich) for 48 h under normoxic conditions to investigate whether the low expression of miR-495 and miR-5688 under hypoxia depended on HIF-1α.

2.2 | Human tissue specimens

Paired human NSCLC tissues and corresponding adjacent normal tissues were obtained from 28 patients during surgical procedure between February 2018 and January 2019 at the Tianjin Medical University Cancer Institute and Hospital (Tianjin, China). Tissue fragments were promptly frozen in liquid nitrogen at the time of surgery and stored at −80°C. Both the tumor and noncancerous tissues were histologically confirmed. The pathological type of each tumor was determined to be adenocarcinoma. None of the patients received chemotherapy or radiotherapy prior to surgery. In addition, no malignancy in other organs was reported prior to surgery. The mRNA expression levels of miR-495, miR-5688, and IL-11 in 28 pairs of clinical samples were examined. All samples were obtained with informed consent, and the study was approved by the Ethics Committee of Tianjin Medical University Cancer Institute and Hospital.

2.3 | Plasmid construction and transfection

To generate the miR-495 and miR-5688 overexpression plasmids (pri-miR-495 and pri-miR-5688), 414 bp and 415 bp fragments containing the miR-495- and miR-5688-coding regions were amplified from genomic DNA and cloned into the pcDNA3.1 vector (Ambion, Austin, TX, USA) at the EcoR I and BamH I sites. The 2′-O-methyl-modified miR-495 and miR-5688 antisense oligonucleotides (ASO-miR-495 and ASO-miR-5688) were commercially synthesized by GenePharma Co., Ltd (Shanghai, China) and used as inhibitors of miR-495 and miR-5688. The 3′-UTR sequences of IL-11 that contain the miR-495-binding and miR-5688-binding sites and mutant 3′-UTR fragments with mutated miR-495-binding and miR-5688-binding sites were obtained by annealing double-stranded DNA and inserting it into the pmirGLO vector (Promega, Madison,WI, USA). The sequences of all primers for PCR amplification are provided in **Table 1**.

2.4 | Construction of stable cell lines for establishing NSCLC xenograft model

miR-495 and miR-5688 expression lentiviruses were obtained from Genechem Co., Ltd (Shanghai, China). A549 cells, which have better tumorigenicity than H1299 cells, were incubated with virus supernatants for 12 h with 8 µg/mL polybrene (Solarbio, Beijing, China) following the manufacturer's instructions. Infected cells were selected with puromycin (Sigma-Aldrich).

TABLE 1 Sequences of primers used in this study

Primer	Sequences
Plasmid construct primer	
miR-495 sence	5′-CGCGGATCCAACTTACCTGATGCTTTTAGGCTTA-3′
miR-495 antisence	5′-CCGGAATTCCTCGCCAACTGTGCCTGT-3′
miR-5688 sence	5′-CGCGGATCCTGTTTTATGAGGTTGGGCTAT-3′
miR-5688 antisence	5′-CCGGAATTCCAAAATGAATATGTGTACTATGCTC-3′
IL-11 3′-UTR-WT sence	5′-CCCCGCACTGCATAGGGCCTTTTGTTTGTTTTTTGAGAT-3′
IL-11 3′-UTR-WT antisence	5′-CTAGATCTCAAAAAACAAACAAAAGGCCCTATGCAGTGCGGGGAGCT-3′
IL-11 3′-UTR-MUT sence	5′-CCCCGCACTGCATAGGGCCTTTTATCGGGCTTTTGAGAT-3′
IL-11 3′-UTR-MUT antisence	5′-CTAGATCTCAAAAGCCCGATAAAAGGCCCTATGCAGTGCGGGGAGCT-3′
quantitative RT-PCR primer	
miR-495 RT	5′-GTCGTATCCAGTGCAGGGTCCGAGGTGCACTGGATACGACAAGAAGT-3′
miR-5688 RT	5′-GTCGTATCCAGTGCAGGGTCCGAGGTGCACTGGATACGACGCTGTTT-3′
U6 RT	5′-GTCGTATCCAGTGCAGGGTCCGAGGTATTCGCACTGGATACGACAAAATATGGAAC-3′
miR-495 forward	5′-TGCGGAAACAAACATGGTGC-3′
miR-5688 forward	5′-TGCGGTAACAAACACCTGTA-3′
U6 forward	5′-TGCGGGTGCTCGCTTCGGCAGC-3′
microRNA reverse	5′-CCAGTGCAGGGTCCGAGGT-3′
IL-11 forward	5′-CGAGCGGACCTACTGTCCTA-3′
IL-11 reverse	5′-GCCCAGTCAAGTGTCAGGTG-3′
GAPDH forward	5′-GGAGCGAGATCCCTCCAAAAT-3′
GAPDH reverse	5′-GGCTGTTGTCATACTTCTCATGG-3′

Abbreviations: miR, microRNA; IL-11, interleukin-11; 3′-UTR, 3′-untranslated region; WT, wild-type; MUT, mutant; RT, reverse transcription; GAPDH, glyceraldehyde-3-phosphate dehydrogenase.

2.5 | Cell proliferation assay

A549 and H1299 cells (5000 cells per well) were seeded in 96-well plates 1 day prior to transfection and then transfected with pri-miRNAs, ASO-miRNAs, or the respective controls using lipofectamine 2000 reagent (Invitrogen, Camarillo, CA, USA) according to the manufacturer's protocol. 24 h later, 20 µL of 0.5 mg/mL 3-(4,5-dimethylthiazol-2-yl)-5-(3-carboxymethoxyphenyl)-2-(4-sulfophenyl)-2H-tetrazolium (MTS) reagent (Promega) was added to each well. The cells were incubated at 37°C for 1 h. Next, the absorbance at 570 nm was detected at 0, 48, and 72 h after transfection on a μQuant Universal Microplate Spectrophotometer (Bio-Tek Instruments, Winooski, VT, USA). Then, we processed these data to generate cell proliferation curves using Graphpad Prism 6.

2.6 | Colony formation assay

At 24 h after transfection, A549 and H1299 cells were seeded into 6-well plates at a density of 400 cells per well using RPMI-1640 supplemented with 10% FBS. The medium was replaced every two days. When most cell clumps achieved > 50 cells, as observed under a microscope (Olympus, Tokyo, Japan), the colonies were then fixed with paraformaldehyde (Solarbio), stained with crystal violet (Solarbio), and counted.

2.7 | Wound healing assay

At 24 h after transfection, A549 and H1299 cells were cultured in 6-well plates at a density of approximately 5 × 10^5 cells per well. When cell confluence reached approximately 95%-100%, scratches were generated using a 100-µL pipette tip. Non-adherent cells were removed by PBS washes. The cells were incubated in medium containing 5% FBS for 0, 24, and 48 h. Five fields of view for each well were randomly captured at × 100 magnification under the microscope (Olympus) to prevent uneven cell distribution which could otherwise result in false negatives or false positives.

2.8 | Transwell assay

A549 and H1299 cells were placed on the upper chamber of each insert coated with 40 µL of Matrigel (BD Biosciences,

TABLE 2 Associations between miR-495 and miR-5688 expression levels and clinicopathological characteristics of 28 NSCLC patients

Characteristics	Total (cases)	Expression of miR-495 (cases)			Expression of miR-5688 (cases)		
		Low	High	*P* value	Low	High	*P* value
Total	28	14 (50.0%)	14 (50.0%)		17 (60.7%)	11 (39.3%)	
Age (years)				0.128			0.254
< 60	13	4 (30.8%)	9 (69.2%)		10 (76.9%)	3 (23.1%)	
≥60	15	10 (66.7%)	5 (33.3%)		7 (46.7%)	8 (53.3%)	
Gender				0.440			0.701
Male	17	7 (41.2%)	10 (58.8%)		11 (64.7%)	6 (35.3%)	
Female	11	7 (63.6%)	4 (36.4%)		6 (54.5%)	5 (45.5%)	
Smoking history				0.695			0.444
Present	10	6 (60.0%)	4 (40.0%)		5 (50.0%)	5 (50.0%)	
Absent	18	8 (44.4%)	10 (55.6%)		12 (66.7%)	6 (33.3%)	
Family history of cancer				0.420			0.249
Present	9	6 (66.7%)	3 (33.3%)		7 (77.8%)	2 (22.2%)	
Absent	19	8 (42.1%)	11 (57.9%)		10 (52.6%)	9 (47.4%)	
Tumor size (cm)				0.033[*]			0.030[*]
< 5	8	1 (12.5%)	7 (87.5%)		2 (25.0%)	6 (75.0%)	
≥5	20	13 (65.0%)	7 (35.0%)		15 (75.0%)	5 (25.0%)	
Tumor differentiation				0.008[**]			0.002[**]
Poor	12	10 (83.3%)	2 (16.7%)		11 (91.7%)	1 (8.3%)	
Moderate	9	3 (33.3%)	6 (66.7%)		5 (55.6%)	4 (44.4%)	
Well	7	1 (14.3%)	6 (85.7%)		1 (14.3%)	6 (85.7%)	
TNM stage stagstageclassification				0.007[**]			0.012[*]
I	6	1 (16.7%)	5 (83.3%)		3 (50.0%)	3 (50.0%)	
II	7	1 (14.3%)	6 (85.7%)		1 (14.3%)	6 (85.7%)	
III	8	7 (87.5%)	1 (12.5%)		7 (87.5%)	1 (12.5%)	
IV	7	5 (71.4%)	2 (28.6%)		6 (85.7%)	1 (14.3%)	
Lymph node metastasis				0.165			0.174
Present	22	13 (59.1%)	9 (40.9%)		15 (68.2%)	7 (31.8%)	
Absent	6	1 (16.7%)	5 (83.3%)		2 (33.3%)	4 (66.7%)	
Distant metastasis				0.192			0.381
Present	7	5 (71.4%)	2 (28.6%)		3 (42.9%)	4 (57.1%)	
Absent	21	9 (42.9%)	12 (57.1%)		14 (66.7%)	7 (33.3%)	

Differences between experimental groups were assessed by Fisher's exact probability test. Data represent mean ± standard deviation. *$P < 0.05$; **$P < 0.01$.

San Jose, CA, USA), which was diluted to 4 μg/μL with serum-free medium. Then, medium supplemented with 20% FBS (600 μL) was added to the lower chamber. After 24-hour incubation at 37°C, the upper surface of the membrane was wiped with a cotton tip, and the cells attached to the lower surface were stained for 15 min with crystal violet. Cells in five random fields of view at × 100 magnification were counted and expressed as the average number of cells per field of view. All assays were performed in triplicate.

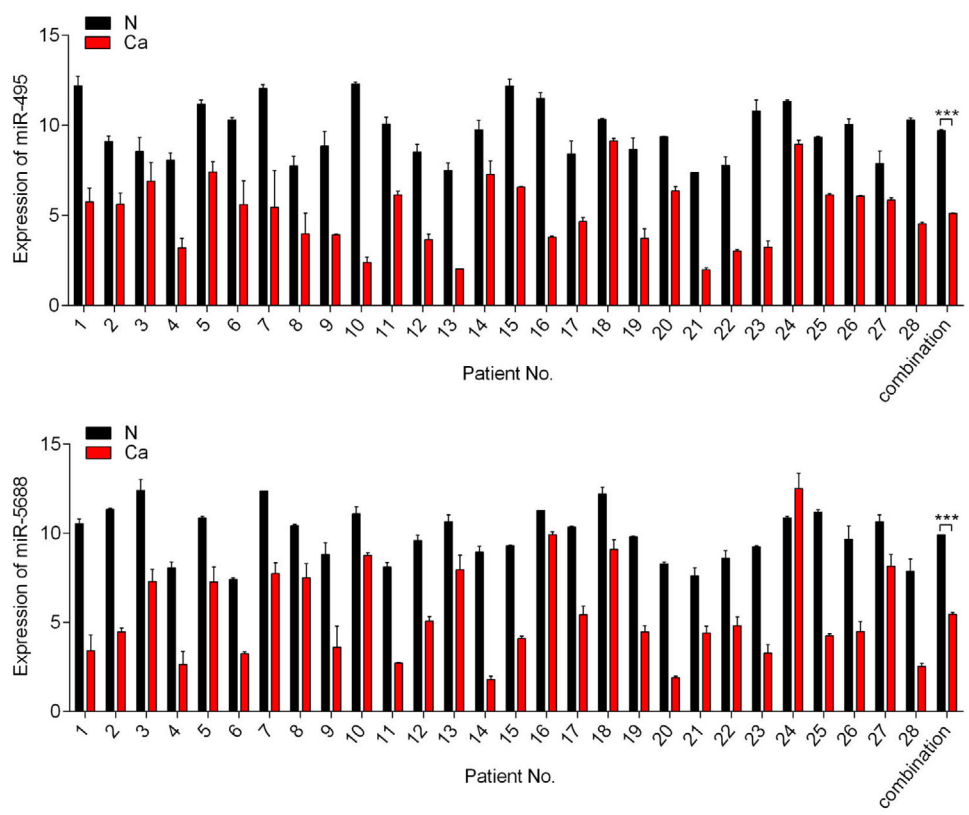## 2.9 | Prediction of miRNA targets

The potential targets of miR-495 and miR-5688 were predicted using TargetScan 7.2 (http://www.targetscan.org/) and PicTar (http://pictar.mdc-berlin.de/).
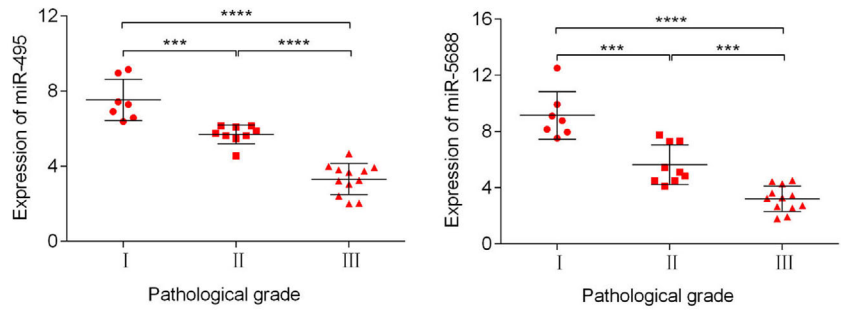
2.10 | Luciferase reporter assay

A549 and H1299 cells were seeded in 24-well plates 1 day before transfection at a density of 1.2×10^5 cells per well
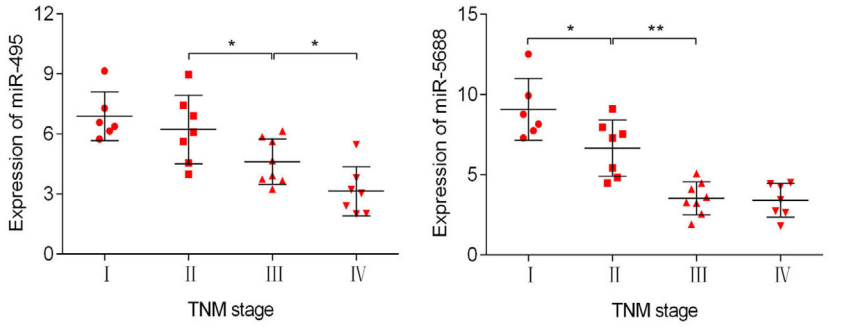
a

b

c

and were then co-transfected with 2 pmol of pri-miRNAs, ASO-miRNAs, or their respective negative control and equal doses (2 mg) of pmirGLO-IL-11 3′-UTR-wild-type (WT) or pmirGLO-IL-11 3′-UTR-mutant (MUT) using Lipofectamine 2000 (Invitrogen). After transfection for 48 h, firefly and renilla luciferase activities were measured using the Dual Luciferase Assay System (Promega). Each reporter plasmid was transfected at least twice (on different days), and each sample was assayed in triplicate.

2.11 | IL-11 concentration

The IL-11 concentration in cell culture supernatants was determined by a human IL-11 immunoassay ELISA kit (R&D Systems, Minnesota, MN, USA). The assay was performed as previously described [21]. Briefly, 100 μL of assay diluent and 100 μL of standard or sample per well were added to the microplate and incubated for 2 h. After washing 4 times with the washing buffer supplied by the kit, the microplate was incubated with 200 μL of IL-11 conjugate for 3 h. After another 4 washes, 200 μL of substrate solution was added and incubated for 30 min. The absorbance of all wells was determined at 450 nm to evaluate the concentration of IL-11.

2.12 | qRT-PCR

Total RNA was isolated using TRIzol reagent (Invitrogen). Total RNA (2 μg) was used for the synthesis of first-strand cDNA using M-MLV reverse transcriptase (Invitrogen). Quantitative real-time PCR was performed using SYBR Green Mix (Cwbiotech, Beijing, China). The reactions were performed with a real-time fluorescent PCR instrument (Roche, Basel, Switzerland). The data are displayed as $2^{-\triangle\triangle Ct}$ values and are representative of at least three independent experiments. Sequences of the qRT-PCR primers are provided in Table 1.

2.13 | Western blotting analysis

Cell extracts were prepared with radioimmunoprecipitation assay (RIPA) lysis buffer (Millipore, Bedford, MA, USA). The cell lysates were incubated at 4°C for 1 h with rotation, followed by clarification of cell debris by centrifugation at 12,000 rpm for 10 min. The protein concentration was determined using the BCA Protein Assay Kit (Thermo Fisher Scientific, Basingstoke, UK). Antibodies against HIF-1α (1:1000, Abcam), IL-11 (1:1000, Abcam), and glyceraldehyde-3-phosphate dehydrogenase (GAPDH, 1:5000, Abcam) were used for protein detection. Antibody complexes were detected using the Immobilon Western Chemiluminescent HRP Substrate (Millipore) and Amersham Imager 600 (GE Healthcare, Beijing, China).

2.14 | NSCLC xenograft model

Thirty-three female athymic nude mice (BALB/c-nu) were purchased from the Academy of Military Medical Science (Beijing, China). All mouse studies were approved by the Animal Ethics Committee of Tianjin Medical University. All mice were 4-5 weeks of age at the time of injection. A549-vector, A549-pri-miR-495, or A549-pri-miR-5688 cells and A549 cells transfected with ASO-NC or ASO-miRNAs were trypsinized, washed, resuspended in Hanks' balanced salt solution (HBSS; Gibco), and injected into the right flanks subcutaneously (5×10^6 cells/animal). Mice were euthanized 3-4 weeks after inoculation. Then, the weight of the subcutaneous tumors was recorded and used to determine tumor growth or suppression.

2.15 | Statistical analyses

The SPSS 19.0 software (IBM Corp., Armonk, NY, USA) was employed to perform statistical analyses. Data are reported as the mean ± standard deviation (SD). Biochemical experiments were performed in triplicate, and a minimum of three independent experiments were analyzed. Differences were assessed for statistical significance by an unpaired two-tailed t test and Fisher's exact probability test. Pearson correlation analysis was used to analyze the correlation between the expression of miR-495 or miR-5688 and the pathological grade or TNM stage (classified according to the 7th edition of the Union for International

FIGURE 1 miR-495 and miR-5688 are down-regulated in human non-small cell lung cancer (NSCLC). (a) The expression levels of miR-495 and miR-5688 in 28 pairs of NSCLC tissues (Ca) and matched adjacent normal tissues (N) were detected by quantitative real-time polymerase chain reaction (qRT-PCR). U6 snRNA was used as an endogenous normalization control. (b) Expression of miR-495 and miR-5688 in NSCLC patients with different pathological grades. (c) Expression of miR-495 and miR-5688 in NSCLC patients with different TNM stages. All of the experiments were repeated three times. Differences between groups were analyzed by using the unpaired t-test (*$P < 0.05$; **$P < 0.01$; ***$P < 0.001$; ****$P < 0.0001$)
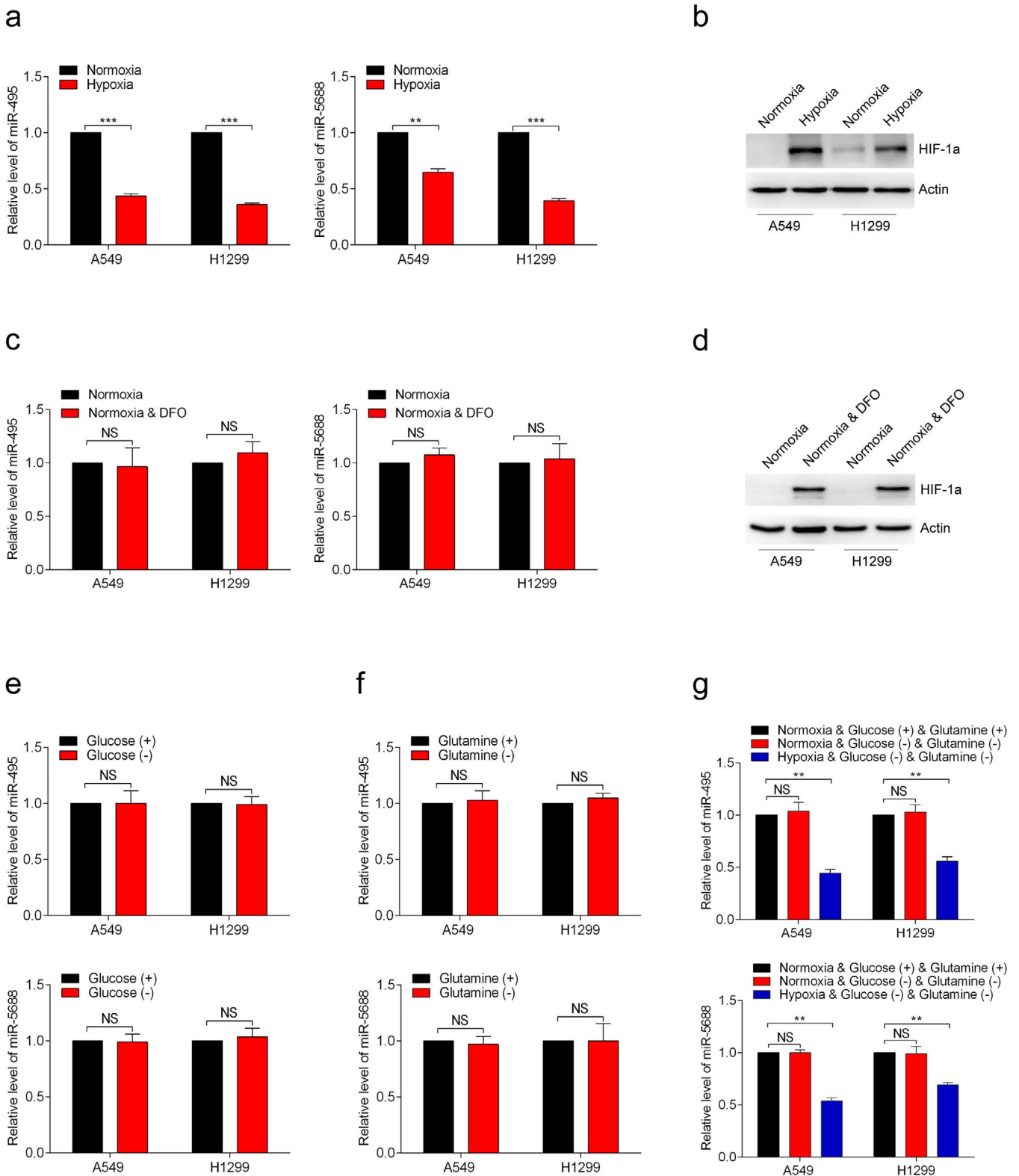
FIGURE 2 The hypoxic microenvironment leads to the down-regulation of miR-495 and miR-5688 in NSCLC. (a) A549 and H1299 cells were cultured under hypoxic conditions (0.5% O_2) or normoxic conditions for 48 h. Then, the expression levels of miR-495 and miR-5688 were determined by qRT-PCR. (b) The expression of HIF-1α was determined by Western blotting in A549 and H1299 cells under normoxia and hypoxia. (c) The expression levels of miR-495 and miR-5688 were determined by qRT-PCR in A549 and H1299 cells treated with DFO (100 μmol/L) for 48 h under normoxic conditions. (d) The expression of HIF-1α was determined by Western blotting in A549 and H1299 cells treated with DFO under normoxia. (e) A549 and H1299 cells were cultured in normal glucose medium and glucose-free medium for 48 h, and the expression levels of miR-495 and miR-5688 were detected by qRT-PCR. (f) A549 and H1299 cells were cultured in normal glutamine medium

Cancer Control TNM staging system) of NSCLC. A *P* value less than 0.05 was considered significant.

3 | RESULTS

3.1 | miR-495 and miR-5688 are down-regulated in NSCLC tissues

The clinicopathological features of the 28 patients are listed in the Table 2. We examined the expression levels of miR-495 and miR-5688 in 28 pairs of human NSCLC tissues and adjacent normal tissues using qRT-PCR. miR-495 and miR-5688 expression levels were generally lower in NSCLC tissues than in matched normal tissues (Figure 1a), suggesting that miR-495 and miR-5688 were down-regulated in NSCLC. The expression of miR-495 or miR-5688 was negatively correlated with pathological grade (miR-495, $r = -0.909$; miR-5688, $r = -0.882$; Figure 1b) and TNM stage of NSCLC (miR-495, $r = -0.745$; miR-5688, $r = -0.818$; Figure 1c). These results might highlight the potential of miR-495 and miR-5688 in predicting the prognosis of NSCLC.

3.2 | Hypoxic microenvironment leads to the down-regulation of miR-495 and miR-5688 in NSCLC tissues

To further investigate the reasons for the low expression of miR-495 and miR-5688 in NSCLC, we examined whether the expression of miR-495 and miR-5688 changed in different tumor microenvironments. We cultured A549 and H1299 cells under hypoxic conditions (0.5% O_2) and found that the expression levels of miR-495 and miR-5688 were decreased compared with those in normoxic cells (Figure 2a). Western blotting analysis demonstrated that hypoxia stimulation induced HIF-1α expression in both A549 and H1299 cells, indicating the successful establishment of hypoxia (Figure 2b). When treated with DFO for 48 h, the expression levels of miR-495 and miR-5688 did not change (Figure 2c), and the expression of HIF-1α was stable in A549 and H1299 cells (Figure 2d), suggesting that the expression of miR-495 and miR-5688 were independent on HIF-1α.

Next, we cultured the A549 and H1299 cells in glucose-free medium for 48 h and found that glucose deficiency did not affect the expression of miR-495 and miR-5688

(Figure 2e). Similar results were obtained when glutamine was absent from the cell culture medium in A549 and H1299 cells (Figure 2f). Then, we further explored whether the expression of miR-495 and miR-5688 in A549 and H1299 cells would be altered in the absence of both glucose and glutamine. As depicted in Figure 2g, the expression of miR-495 and miR-5688 remained unchanged. However, after 48 h of hypoxia treatment using the same culture medium, the expression levels of miR-495 and miR-5688 were decreased significantly (Figure 2g). These results indicated that the hypoxia-mediated down-regulation of miR-495 and miR-5688 was caused directly by low oxygen level.

3.3 | miR-495 and miR-5688 inhibit NSCLC cell proliferation *in vitro* and tumor formation *in vivo*

To investigate the role of miR-495 and miR-5688 in NSCLC cells, gain- and loss-of-function assays were performed in A549 and H1299 cells. qRT-PCR showed that pri-miR-495 and pri-miR-5688 resulted in a 6- to 7-fold increase in the expression levels of miR-495 and miR-5688. Conversely, ASO-miR-495 and ASO-miR-5688 reduced miR-495 and miR-5688 levels by 60%-70% relative to the controls (Figure 3a). In addition, MTS assays showed that the over-expression of miR-495 or miR-5688 reduced the viability of A549 and H1299 cells, whereas the inhibition of miR-495 or miR-5688 led to increased cell viability (Figure 3b). The colony-formation rates of A549 and H1299 cells were decreased by pri-miR-495 and increased by ASO-miR-495. Similar results were observed in A549 and H1299 cells transfected with pri-miR-5688 and ASO-miR-5688 (Figure 3c). Together, these data indicated that miR-495 and miR-5688 inhibited NSCLC cell proliferation *in vitro*.

To further validate the effects of miR-495 and miR-5688 on the malignant phenotype of NSCLC, we conducted a xenograft tumor formation assay. The transfection of pri-miR-495 and pri-miR-5688 significantly inhibited the growth of xenograft tumors in nude mice (Figure 3d) and suppressed IL-11 expression in xenograft tumors (Figure S1a). Conversely, the transfection of ASO-miR-495 and ASO-miR-5688 promoted the tumor formation ability of A549 cells (Figure S1b) and up-regulated the expression of IL-11 in xenografts (Figure S1c). These results demonstrated that miR-495 and miR-5688 inhibited NSCLC tumor formation in vivo.

and glutamine-free medium for 48 h, and the expression levels of miR-495 and miR-5688 were detected by qRT-PCR. (g) The expression levels of miR-495 and miR-5688 in A549 and H1299 cells were detected by qRT-PCR after 48 h of culture under normoxia and hypoxia using medium free of glucose and glutamine. All of the experiments were repeated three times. Differences between groups were analyzed by using the unpaired *t*-test (**$P < 0.01$; ***$P < 0.001$; NS, not significant)
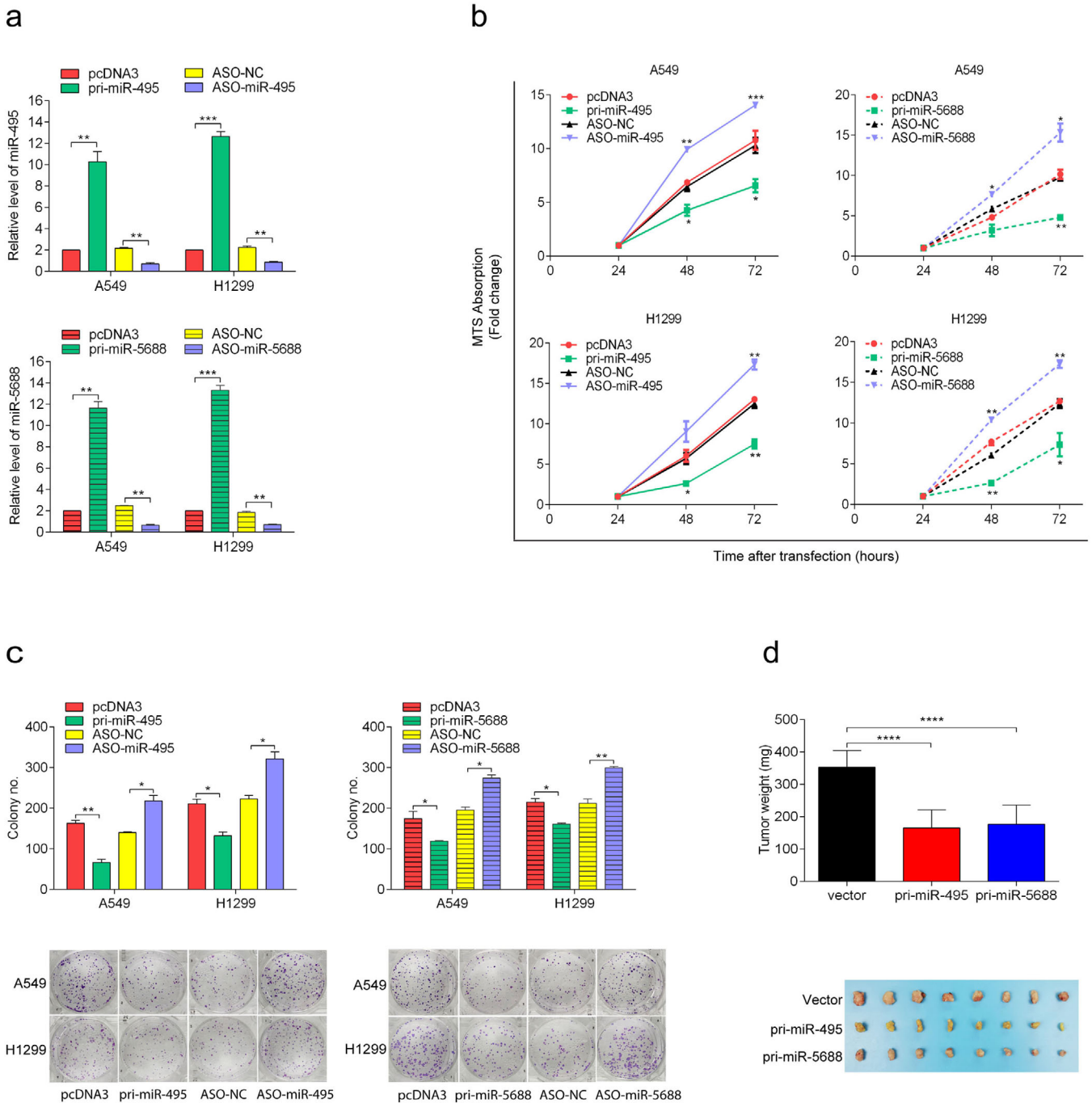
FIGURE 3 miR-495 and miR-5688 inhibit NSCLC cell proliferation in vitro and tumor formation in vivo. (a) Relative levels of miR-495 and miR-5688 after transfection with pri-miR-495, pri-miR-5688, ASO-miR-495, ASO-miR-5688, or their respective controls in A549 and H1299 cells. The data are shown as the means ± standard deviation (SD) ($n = 3$). (b) Proliferation curves of A549 and H1299 cells were determined at 48 h and 72 h by MTS assay after transfection with pri-miR-495, pri-miR-5688, ASO-miR-495, ASO-miR-5688, or their respective controls. The data are shown as the means ± SD ($n = 3$). (c) Colony formation of A549 and H1299 cells infected with pri-miR-495, pri-miR-5688 or ASO-miR-495, ASO-miR-5688, or their respective controls. The data are shown as the means ± SD ($n = 3$). (d) Female nude mice were injected with A549-vector, A549-pri-miR-495, or A549-pri-miR-5688 cells into the right flanks subcutaneously (5×10^6 cells/animal) and were euthanized 4 weeks after injection. The average tumor weights are presented in the bar graphs (means ± SD; $n = 8$ for each group). Differences between groups were analyzed by unpaired t-test (*$P < 0.05$; **$P < 0.01$; ***$P < 0.001$; ****$P < 0.0001$)
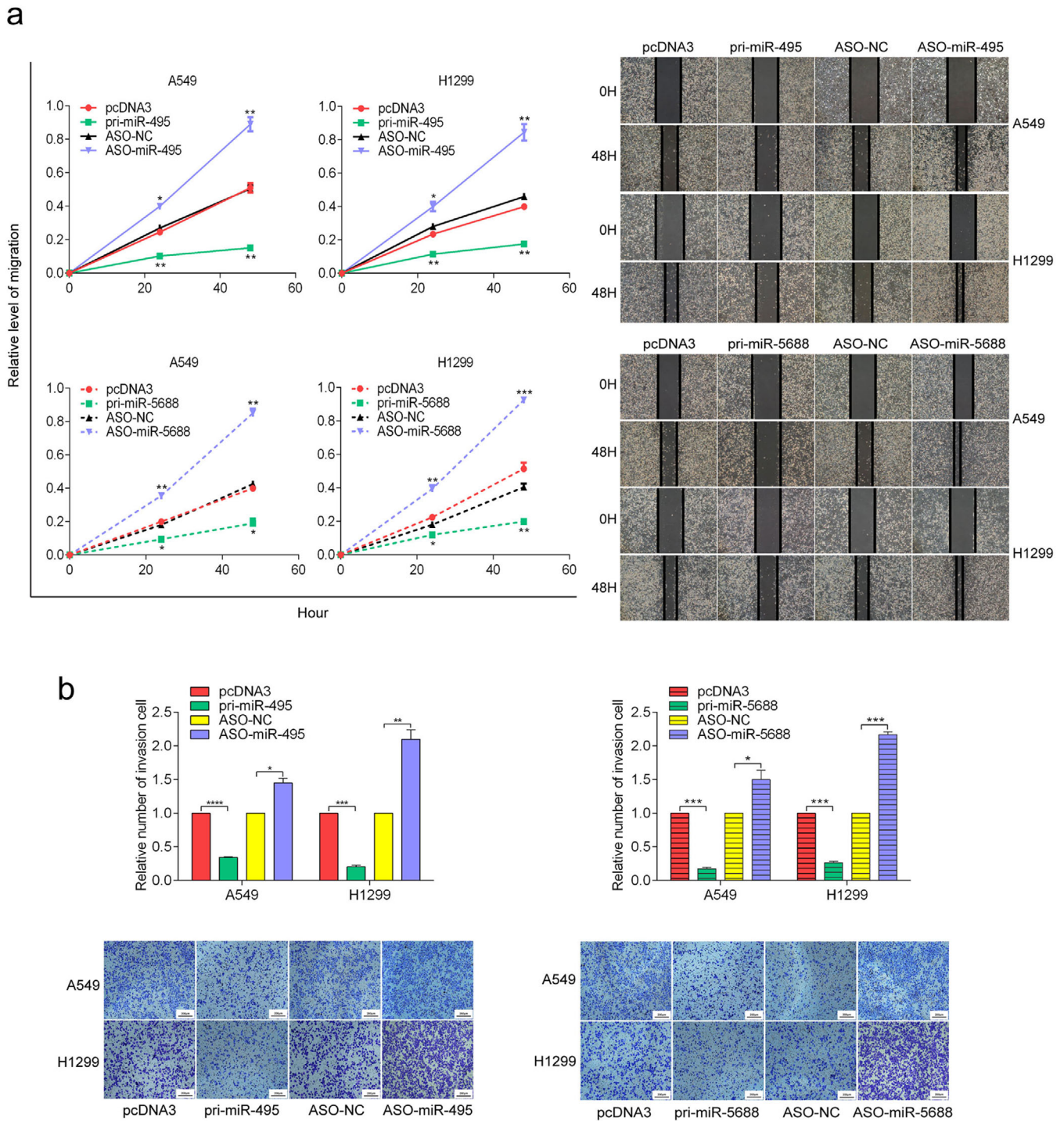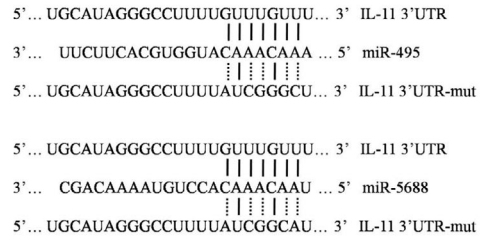
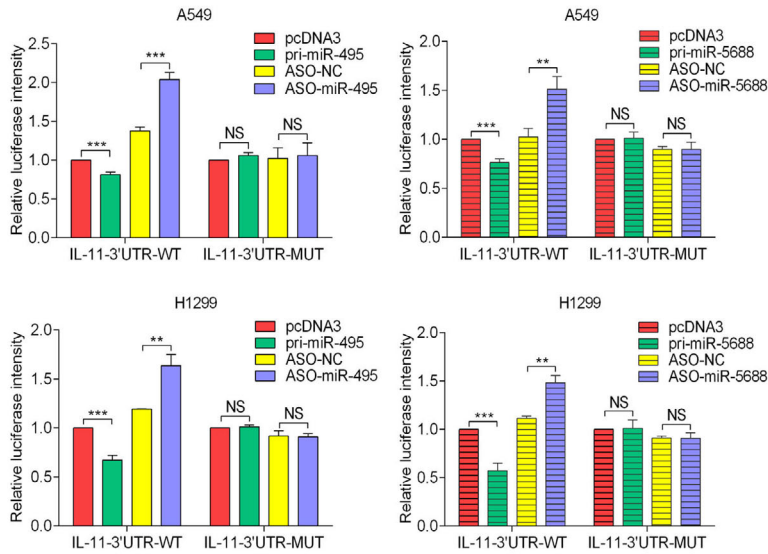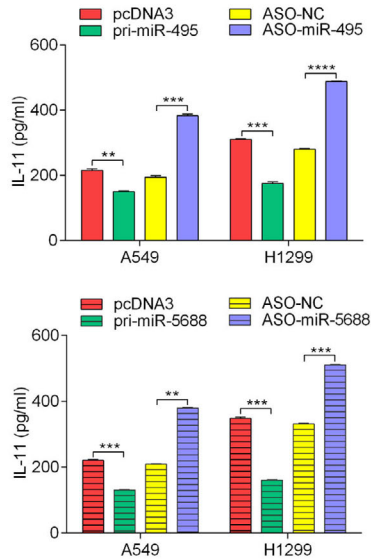**FIGURE 4** miR-495 and miR-5688 inhibit NSCLC cell migration and invasion in vitro. (a) Wound healing assays for A549 and H1299 cells infected with pri-miR-495, pri-miR-5688, ASO-miR-495, ASO-miR-5688, or their respective controls were used to measure migration at 24 h and 48 h, and the quantitative patterns are shown. (b) Assay of the invasion of A549 and H1299 cells infected with pri-miR-495, pri-miR-5688, ASO-miR-495, ASO-miR-5688, or their respective controls. All of the experiments were repeated three times. Differences between groups were analyzed by unpaired t-test (*$P < 0.05$; **$P < 0.01$; ***$P < 0.001$; ****$P < 0.0001$)

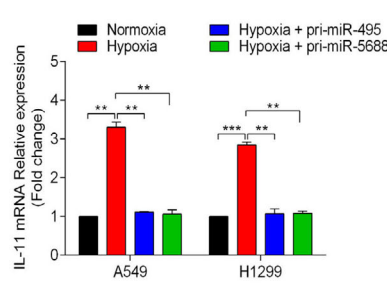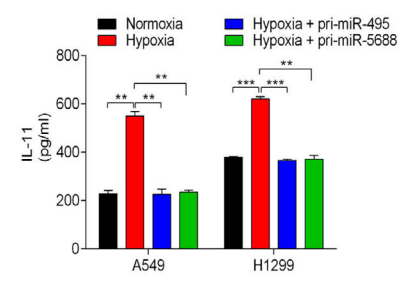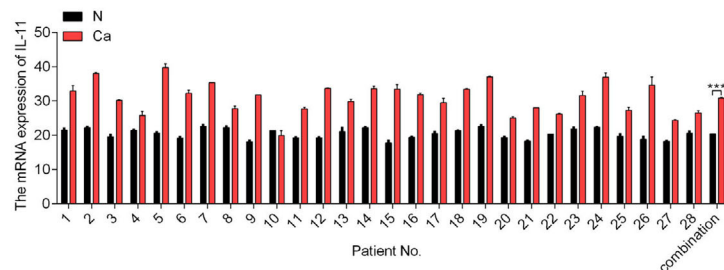## 3.4 | miR-495 and miR-5688 inhibit NSCLC cell migration and invasion *in vitro*

We subsequently explored the role of miR-495 and miR-5688 in invasion and metastasis. Wound healing assays revealed that the migration of A549 and H1299 cells was significantly inhibited by pri-miR-495 and pri-miR-5688 but promoted by ASO-miR-495 and ASO-miR-5688 (Figure 4a). In addition, transwell assay results demonstrated similar effects of miR-495 and miR-5688 on cell invasion (Figure 4b). Taken together, these results indicated that miR-495 and miR-5688 inhibited NSCLC cell migration and invasion *in vitro*.

3.5 | miR-495 and miR-5688 directly target IL-11 and reverse the increased IL-11 expression due to hypoxia in NSCLC cells

To investigate the underlying molecular mechanisms by which miR-495 and miR-5688 exert their anti-tumor effects, we screened for putative miR-495 and miR-5688 targets using bioinformatics methods. Target prediction suggested hundreds of candidate targets for miR-495 and miR-5688, and we chose IL-11 as a putative target for further study after considering the available functional data (Figure 5a). To validate whether IL-11 is directly targeted by miR-495 and miR-5688, we performed a luciferase assay using luciferase reporter vectors containing either the 3'-UTR-WT or a 3'-UTR-MUT with a mutation in the complementary miRNA binding sequence of IL-11 (Figure 5b). In A549 and H1299 cells, pri-miR-495 and pri-miR-5688 significantly decreased the luciferase activity of the pmirGLO-IL-11 3'-UTR, whereas ASO-miR-495 and ASO-miR-5688 significantly enhanced the luciferase activity of the pmirGLO-IL-11 3'-UTR). However, luciferase activity of the mutant 3'-UTR of IL-11 was not influenced by either over-expression or inhibition of miR-495 and miR-5688 (Figure 5c). These results suggested that IL-11 was a direct target of miR-495 and miR-5688.
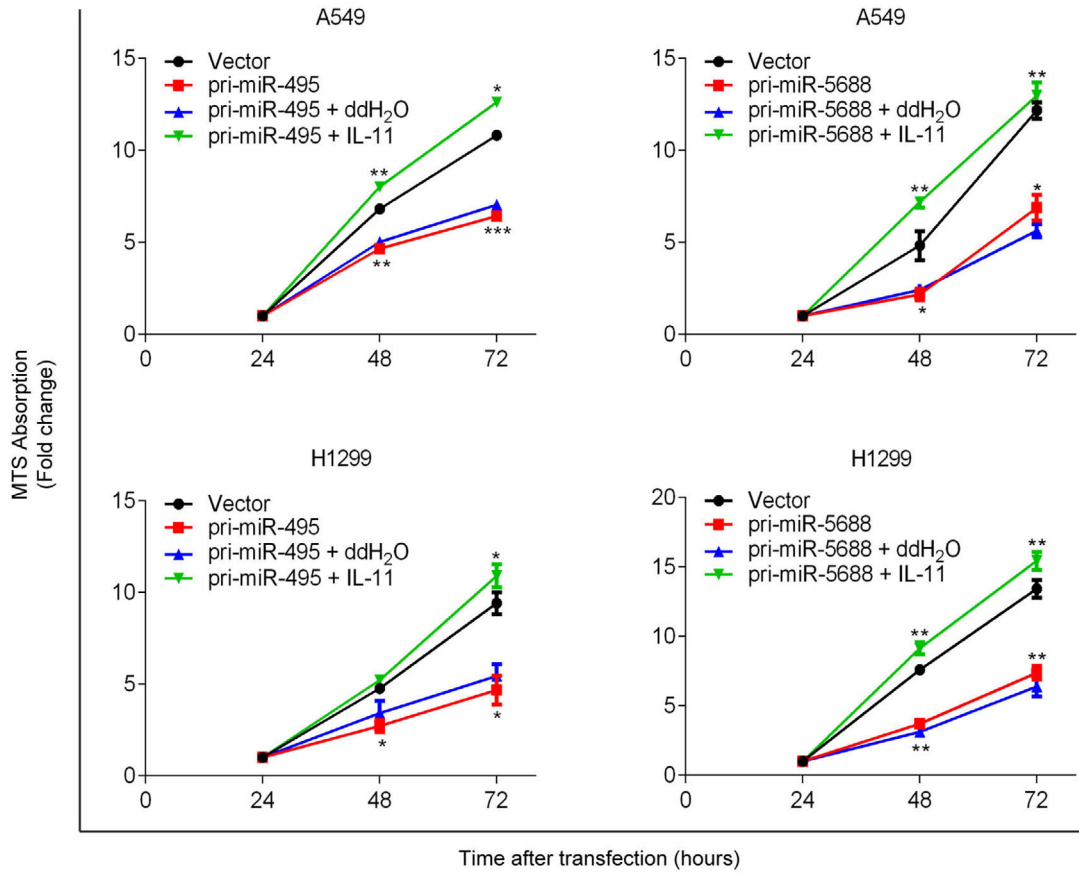
Next, we determined the effects of miR-495 and miR-5688 on endogenous IL-11 expression. qRT-PCR showed that the IL-11 mRNA level was decreased in A549 and H1299 cells transfected with pri-miR-495 and pri-miR-5688 (Figure 5d). In addition, ELISA results showed that the secretion of IL-11 was significantly reduced in these cells (Figure 5e). Conversely, cells transfected with ASO-miR-495 and ASO-miR-5688 showed the opposite results (Figure 5d and 5e). These results showed that miR-495 and miR-5688 down-regulated the expression of IL-11. Furthermore, we know that hypoxia caused the down-regulation of miR-495 and miR-5688 in NSCLC cells. Therefore, we further explored whether the effects of miR-495 and miR-5688 on IL-11 expression still exist under hypoxia. We found miR-495 and miR-5688 reversed the up-regulation of IL-11 expression induced by hypoxia in A549 and H1299 cells (Figure 5f and 5g). In addition, we examined the expression level of IL-11 in 28 pairs of human NSCLC tissues and adjacent normal tissues using qRT-PCR. We found that the IL-11 expression level was generally higher in NSCLC tissues than in matched normal tissues (Figure 5h). These results indicated that IL-11 was directly targeted by miR-495 and miR-5688 in NSCLC cells.

3.6 | IL-11 rescues the inhibition of cell proliferation mediated by miR-495 and miR-5688 in NSCLC
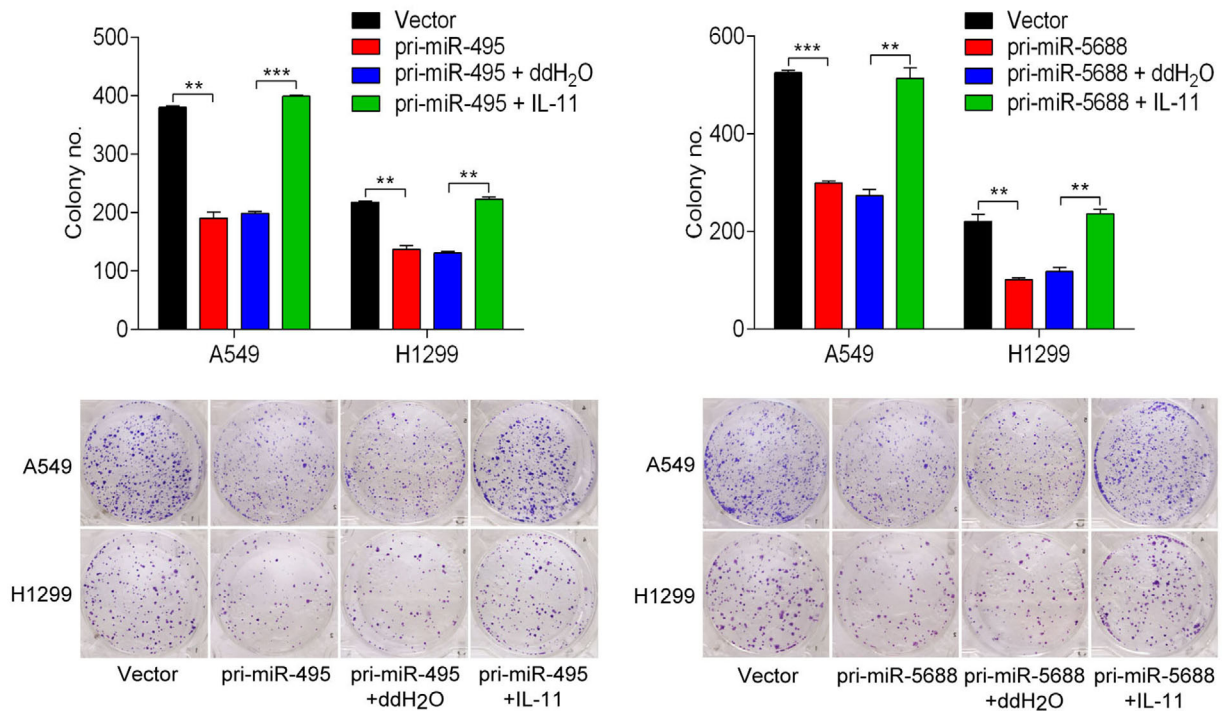
To test whether the effects of miR-495 and miR-5688 expression on cell proliferation, migration, and invasion in A549 and H1299 cells were mediated by IL-11, we performed rescue assays using recombinant human IL-11 in A549 and H1299 cells. We observed that recombinant human IL-11 reversed the decreased proliferation rate of A549 and H1299 cells transfected with pri-miR-495 and pri-miR-5688 (Figure 6a). Furthermore, colony formation assays showed that recombinant human IL-11 rescued the reduced colony formation caused by miR-495 and miR-5688 in A549 and H1299 cells (Figure 6b). Taken together,

FIGURE 5   miR-495 and miR-5688 can directly target IL-11 and reverse the increase in IL-11 expression due to hypoxia in NSCLC cells. (a) The predicted miR-495-binding and miR-5688-binding sites in IL-11 mRNA using Target Scan 7.2 are shown. (b) Wild-type and mutant 3'-UTRs of IL-11 are shown. (c) Luciferase reporters pmirGLO-IL-11 (3'-UTR WT or MUT) were co-transfected with pri-miR-495, pri-miR-5688, ASO-miR-495, ASO-miR-5688, or their respective controls in A549 and H1299 cells. Luciferase activities were measured 48 h post transfection. (d) qRT-PCR shows IL-11 mRNA levels after transfection with pri-miR-495, pri-miR-5688, ASO-miR-495, ASO-miR-5688, or their respective controls in A549 and H1299 cells. (e) ELISA shows the secretion levels of IL-11 after transfection with pri-miR-495, pri-miR-5688, ASO-miR-495, ASO-miR-5688, or their respective controls in A549 and H1299 cells. (f) qRT-PCR shows that hypoxia induced IL-11 expression, which was counteracted by pri-miR-495 and pri-miR-5688. (g) ELISA showed that hypoxia induced IL-11 expression, which is counteracted by pri-miR-495 and pri-miR-5688. (h) The mRNA expression level of IL-11 in 28 pairs of NSCLC tissues and matched adjacent normal tissues was detected by qRT-PCR. All of the experiments were repeated three times. Differences between groups were analyzed by unpaired t-test (*$P < 0.05$; **$P < 0.01$; ***$P < 0.001$; ****$P < 0.0001$; NS, not significant)

a

b

our results suggested that IL-11 counteracted the effects of miR-495 and miR-5688 on cell proliferation.

3.7 | IL-11 rescues the inhibition of cell migration and invasion mediated by miR-495 and miR-5688 in NSCLC

Similarly, we used recombinant human IL-11 to investigate whether the effects of miR-495 and miR-5688 on the migration and invasion of A549 and H1299 cells were mediated by IL-11. Wound healing assays revealed that recombinant human IL-11 disrupted the suppressive effects of miR-495 and miR-5688 on the migration of A549 and H1299 cells (Figure 7a). In addition, transwell assay results showed that recombinant human IL-11 counteracted the effects of miR-495 and miR-5688 (Figure 7b) on the invasion of A549 and H1299 cells.

Furthermore, recombinant human IL-11 rescued the decreased expression levels of miR-495 and miR-5688 in A549 and H1299 cells caused by hypoxia (Figure 7c), suggesting that miR-495 and miR-5688 exerted their activity by regulating IL-11 expression. Collectively, these results suggested that IL-11 could rescue the inhibition of cell migration and invasion mediated by miR-495 and miR-5688.

4 | DISCUSSION

In this study, we identified the miR-495/miR-5688/IL-11 axis as an important mediator in the proliferation, migration, and invasion of NSCLC. At the cellular level, gain- and loss-of function assays indicated that miR-495 and miR-5688 exhibited a tumor suppressive role in NSCLC cells and may be down-regulated due to hypoxia. Mechanistically, both miR-495 and miR-5688 directly targeted the IL-11 transcript 3′-UTR and repressed IL-11 expression.

Hypoxia is a hallmark of the tumor microenvironment [22], leads to resistance to anti-tumor therapy and is associated with a poor prognosis, especially in NSCLC [23, 24]. Various hypotheses have been proposed to explain the tumor promotive role of hypoxia, such as genomic instability, dysfunctional DNA damage repair pathway, and altered transcriptome [24]. In the current study, we demonstrated that miR-495 and miR-5688 were two new players in hypoxia-induced tumor progression. miR-495 and miR-5688 were down-regulated in NSCLC cells under hypoxia

and directly targeted IL-11 mRNA. We previously reported that IL-11 promoted NSCLC progression [21]. Together with the current study, we demonstrated that the miR-495/miR-5488/IL-11 axis was a hypoxia-induced tumor promoter in NSCLC. Furthermore, several lines of evidence have now established miRNAs as key elements in response to hypoxia [25]. For example, the expression changes of the miR-17 family were reported to be involved in the HIF-related response under hypoxia in cancer cells [26]. These data highlight the importance of miRNAs in hypoxia-induced tumor progression.

Over the past few years, hundreds of miRNAs have been described to play important roles in regulating gene expression by mRNA cleavage or translational repression in a variety of model systems [27]. Because of the relative stability of miRNA expression, some studies have used miRNAs as biomarkers [28]. Recent studies have found that miR-495 was involved in the tumorigenesis and progression of various cancers, including lung cancer [11], nasopharyngeal carcinoma [29], osteosarcoma [30], and melanoma [31]. All of these studies have identified miR-495 as a tumor suppressor. Consistent with our findings, it has been reported that miR-495 was expressed at low levels in lung cancer and may act as a tumor suppressor gene [8, 11]. However, the expression and function of miR-5688, which is located in the same cluster as miR-495, is still unclear. Here, we used qRT-PCR to detect the expression levels of miR-495 and miR-5688 in 28 NSCLC tissues and adjacent normal tissues. We found that miR-495 and miR-5688 exhibited low expression in 28 NSCLC tissues compared with adjacent normal tissues. Functional experiments showed that miR-495 and miR-5688 inhibited the proliferation, migration, and invasion of NSCLC. These data suggested that these two miRNAs may be potential biomarkers for NSCLC progression. Whether these two miRNAs can be detected in blood serum needs to be investigated.

IL-11 is a member of the IL-6 family of cytokines, which collectively uses the GP130 signal transduction receptor subunit. It is well known that the classic function of IL-11 is as a hematopoietic growth factor. In recent years, it has been discovered that IL-11 activated the GP130-Janus kinase signaling cascade and the related transcription factor STAT3 by interacting with the ligand-specific IL-11Rα receptor subunit, conferring many of the intrinsic tumor "hallmark" capabilities to neoplastic cells [32]. As reported by Onnis et al. [33], IL-11 is a hypoxia-induced, Von Hippel Lindau (VHL)-regulated gene, and IL-11 expression is

FIGURE 6 IL-11 rescues the inhibition of cell proliferation mediated by miR-495 and miR-5688. (a) MTS assay showed the role of IL-11 in the proliferation of A549 and H1299 cells transfected with pri-miR-495 or pri-miR-5688. (b) Colony formation assays showed the role of IL-11 in the proliferation of A549 and H1299 cells transfected with pri-miR-495 or pri-miR-5688. All of the experiments were repeated three times. Differences between groups were analyzed by unpaired t-test (*$P < 0.05$; **$P < 0.01$; ***$P < 0.001$)

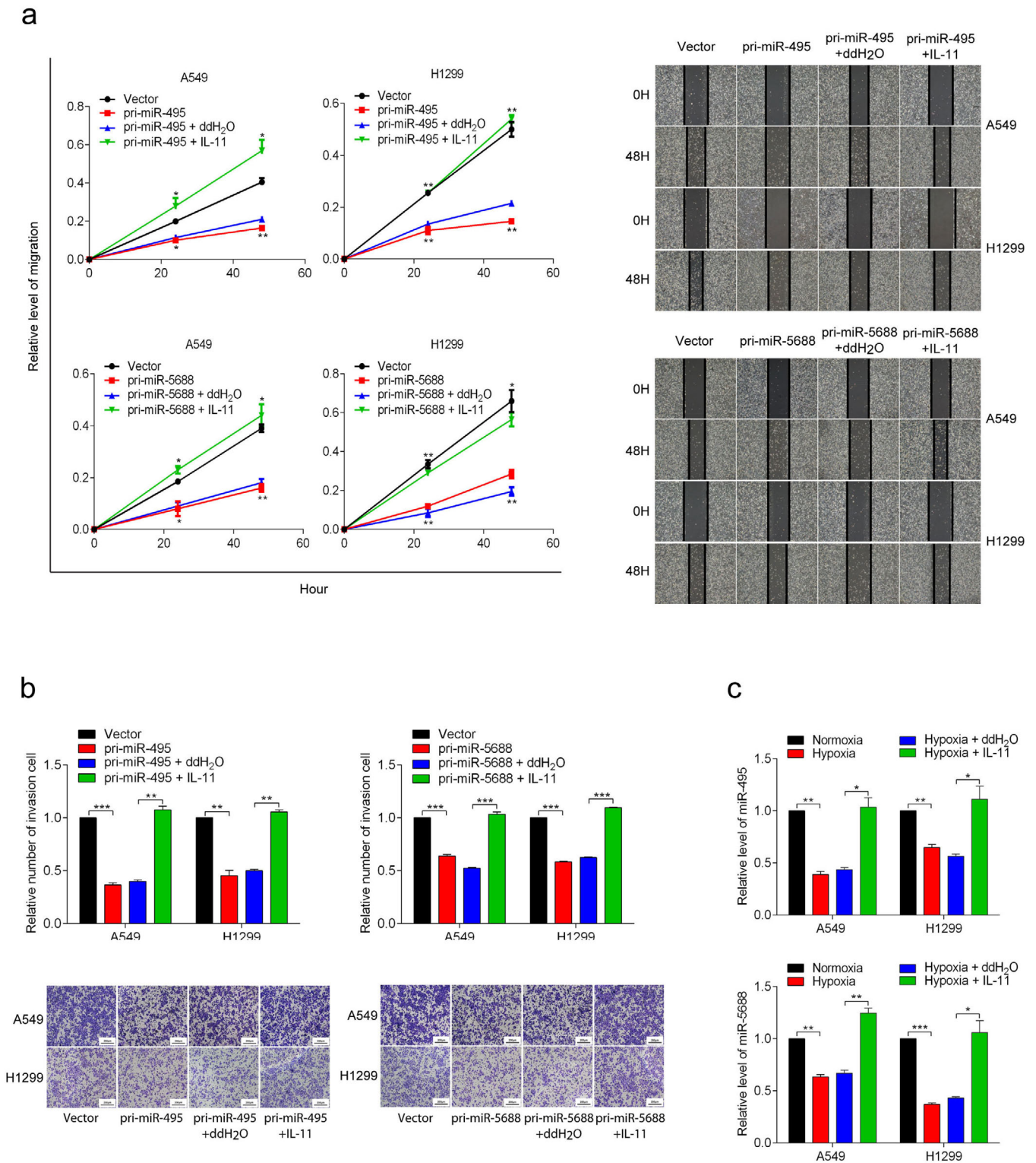**FIGURE 7** IL-11 rescues the inhibition of cell migration and invasion mediated by miR-495 and miR-5688. (a) Wound healing assays showed the role of IL-11 in the migration of A549 and H1299 cells transfected with pri-miR-495 or pri-miR-5688. (b) Transwell assays indicated the role of IL-11 in the invasion of A549 and H1299 cells transfected with pri-miR-495 or pri-miR-5688. (c) The role of IL-11 on the expression of miR-495 and miR-5688 under hypoxia in A549 and H1299 cells is shown. All of the experiments were repeated three times. Differences between groups were analyzed by unpaired t-test (*$P < 0.05$; **$P < 0.01$; ***$P < 0.001$)

partially dependent on HIF-1 in human prostate cancer cells. Our previous research showed that hypoxia up-regulated the expression of IL-11 and promoted the development of NSCLC [21]. In recent years, a growing number of studies have elucidated several miRNAs capable of regulating IL-11 expression in different disease models. For instance, miRNA-124a inhibited cell proliferation and migration in liver cancer by regulating IL-11 [34]. Interestingly, our current study found that IL-11 was a common target of miR-495 and miR-5688. Notably, rescue assays showed that IL-11 could restore the malignant phenotypes suppressed by miR-495 and miR-5688, suggesting that miR-495 and miR-5688 repressed tumorigenic activities by down-regulating IL-11 expression.

5 | CONCLUSIONS

In summary, we demonstrated that hypoxia down-regulated the expression of miR-495 and miR-5688, which promoted the malignancy of NSCLC by up-regulating IL-11 expression. miR-495 and miR-5688 may be used as IL-11 inhibitors for the clinical treatment of NSCLC. However, the detailed mechanism of hypoxia down-regulating the expression of miR-495 and miR-5688 remains unclear, and further studies are needed.

DECLARATION

AUTHOR CONTRIBUTIONS

LR conceived and supervised the project. MZ and JC performed the experiments. RL, YHL, and JQ collected data. YHW and XWZ analyzed the data. MZ and JC wrote the manuscript. LQ, YJ and HHA critically revised the paper. All the authors reviewed the manuscript.

DISCLOSURE STATEMENT

The authors declare that they have no competing interests.

DATA AVAILABILITY STATEMENT

The data that support the findings of this study are available from the corresponding author upon reasonable request.

ORCID

Li Ren https://orcid.org/0000-0001-9675-6184

REFERENCES

1. Gould CM, Courtneidge SA. Regulation of invadopodia by the tumor microenvironment. Cell Adh Migr. 2014;8(3):226-35.
2. Roma-Rodrigues C, Mendes R, Baptista PV, Fernandes AR. Targeting Tumor Microenvironment for Cancer Therapy. Int J Mol Sci. 2019;20(4).
3. Wang M, Zhao J, Zhang L, Wei F, Lian Y, Wu Y, et al. Role of tumor microenvironment in tumorigenesis. J Cancer. 2017;8(5):761-73.
4. Zhang J, Cao J, Ma S, Dong R, Meng W, Ying M, et al. Tumor hypoxia enhances Non-Small Cell Lung Cancer metastasis by selectively promoting macrophage M2 polarization through the activation of ERK signaling. Oncotarget. 2014;5(20):9664-77.
5. Semenza GL. Regulation of Mammalian O2 Homeostasis by Hypoxia-Inducible Factor 1. Annu Rev Cell Dev Biol. 1999;15(1):551-78.
6. Semenza GL. Hypoxia-inducible factors in physiology and medicine. Cell. 2012;148(3):399-408.
7. Torre LA, Siegel RL, Jemal A. Lung Cancer Statistics. Adv Exp Med Biol. 2016;893:1-19.
8. Guo J, Jin D, Wu Y, Yang L, Du J, Gong K, et al. The miR 495-UBE2C-ABCG2/ERCC1 axis reverses cisplatin resistance by downregulating drug resistance genes in cisplatin-resistant non-small cell lung cancer cells. EBioMedicine. 2018;35:204-21.
9. Mao Y, Yang D, He J, Krasna MJ. Epidemiology of Lung Cancer. Surg Oncol Clin N Am. 2016;25(3):439-45.
10. Wakelee H, Kelly K, Edelman MJ. 50 Years of progress in the systemic therapy of non-small cell lung cancer. Am Soc Clin Oncol Educ Book. 2014:177-89.
11. Sun J, Qiao Y, Song T, Wang H. MiR495 suppresses cell proliferation by directly targeting HMGA2 in lung cancer. Mol Med Rep. 2019;19(3):1463-70.
12. Sheng M, Zhao Y, Wang F, Li S, Wang X, Shou T, et al. Targeted drugs for unselected patients with advanced non-small-cell lung cancer: a network meta-analysis. J Thorac Dis. 2016;8(1):98-115.
13. Bartel DP. MicroRNAs: Genomics, Biogenesis, Mechanism, and Function. Cell. 2004;116:281-97.
14. Bartel DP. MicroRNAs: target recognition and regulatory functions. Cell. 2009;136(2):215-33.
15. Zhang PP, Wang XL, Zhao W, Qi B, Yang Q, Wan HY, et al. DNA methylation-mediated repression of miR-941 enhances lysine (K)-specific demethylase 6B expression in hepatoma cells. J Biol Chem. 2014;289(35):24724-35.
16. Tan M, Mu X, Liu Z, Tao L, Wang J, Ge J, et al. microRNA-495 promotes bladder cancer cell growth and invasion by targeting phosphatase and tensin homolog. Biochem Biophys Res Commun. 2017;483(2):867-73.
17. Ye Y, Zhuang J, Wang G, He S, Zhang S, Wang G, et al. MicroRNA-495 suppresses cell proliferation and invasion of hepatocellular carcinoma by directly targeting insulin-like growth factor receptor-1. Exp Ther Med. 2018;15(1):1150-8.
18. Wang L, Liu JL, Yu L, Liu XX, Wu HM, Lei FY, et al. Down-regulated miR-495 [Corrected] Inhibits the G1-S Phase Transition by Targeting Bmi-1 in Breast Cancer. Medicine (Baltimore). 2015;94(21):e718.
19. Negahdaripour M, Nezafat N, Ghasemi Y. A panoramic review and in silico analysis of IL-11 structure and function. Cytokine Growth Factor Rev. 2016;32:41-61.

20. Xu DH, Zhu Z, Wakefield MR, Xiao H, Bai Q, Fang Y. The role of IL-11 in immunity and cancer. Cancer Lett. 2016;373(2):156-63.

21. Zhao M, Liu Y, Liu R, Qi J, Hou Y, Chang J, et al. Upregulation of IL-11, an IL-6 Family Cytokine, Promotes Tumor Progression and Correlates with Poor Prognosis in Non-Small Cell Lung Cancer. Cell Physiol Biochem. 2018;45(6):2213-24.

22. Huang L, Wang W, Hu Z, Guan C, Li W, Jiang X. Hypoxia and lncRNAs in gastrointestinal cancers. Pathol Res Pract. 2019:152687.

23. Salem A, Asselin MC, Reymen B, Jackson A, Lambin P, West CML, et al. Targeting Hypoxia to Improve Non-Small Cell Lung Cancer Outcome. J Natl Cancer Inst. 2018;110(1).

24. Bristow RG, Hill RP. Hypoxia, DNA repair and genetic instability. Nat Rev Cancer. 2008;8(3):180-92.

25. Nallamshetty S, Chan SY, Loscalzo J. Hypoxia: a master regulator of microRNA biogenesis and activity. Free Radic Biol Med. 2013;64:20-30.

26. Serocki M, Bartoszewska S, Janaszak-Jasiecka A, Ochocka RJ, Collawn JF, Bartoszewski R. miRNAs regulate the HIF switch during hypoxia: a novel therapeutic target. Angiogenesis. 2018;21(2):183-202.

27. Hai-Ying Wan L-MG, Tao Liu, Min Liu, Xin Li, Hua Tang. Regulation of the transcription factor NF-B1 by microRNA-9 in human gastric adenocarcinoma. Mol Cancer. 2010;9:16.

28. Hayes J, Peruzzi PP, Lawler S. MicroRNAs in cancer: biomarkers, functions and therapy. Trends Mol Med. 2014;20(8):460-9.

29. Feng X, Lv W, Wang S, He Q. miR495 enhances the efficacy of radiotherapy by targeting GRP78 to regulate EMT in nasopharyngeal carcinoma cells. Oncol Rep. 2018;40(3):1223-32.

30. Zhao G, Zhang L, Qian D, Sun Y, Liu W. miR-495-3p inhibits the cell proliferation, invasion and migration of osteosarcoma by targeting C1q/TNF-related protein 3. Onco Targets Ther. 2019;12:6133-43.

31. Chen G, Xie Y. miR-495 inhibits proliferation, migration, and invasion and induces apoptosis via inhibiting PBX3 in melanoma cells. Onco Targets Ther. 2018;11:1909-20.

32. Johnstone CN, Chand A, Putoczki TL, Ernst M. Emerging roles for IL-11 signaling in cancer development and progression: Focus on breast cancer. Cytokine Growth Factor Rev. 2015;26(5):489-98.

33. Onnis B, Fer N, Rapisarda A, Perez VS, Melillo G. Autocrine production of IL-11 mediates tumorigenicity in hypoxic cancer cells. J Clin Invest. 2013;123(4):1615-29.

34. Yu L, Wang S, Lin X, Lu Y, Gu P. MicroRNA-124a inhibits cell proliferation and migration in liver cancer by regulating interleukin-11. Mol Med Rep. 2018;17(3):3972-8.

SUPPORTING INFORMATION

Additional supporting information may be found online in the Supporting Information section at the end of the article.